Hydrogen fluoride phase behavior and molecular structure: A QM/MM potential model approach

Scott J. Wierzchowski and David A. Kofke
Department of Chemical Engineering, University at Buffalo, The State University of New York, Buffalo, New York 14260-4200

Jiali Gao
Department of Chemistry and Minnesota Supercomputing Institute, University of Minnesota, Minneapolis, Minnesota 55455

(Received 2 June 2003; accepted 17 July 2003)

A molecular-orbital derived polarizable potential function is developed to model liquid and supercritical fluid hydrogen fluoride. The model is based on a novel application of a combined quantum-mechanical and molecular-mechanical (QM/MM) approach, which treats molecular polarization by a semiempirical method. Two geometrical models are examined, differing in the intramolecular bond length for hydrogen fluoride to match values commonly seen in other empirical models. One QM/MM parameter is fit for each model to reproduce the experimental density at one liquid-phase state condition. The models are examined at this state and at one supercritical state condition. Results for the density, radial distribution function, and average molecular dipole moment are considered in comparison to experiment. Also vapor-liquid coexistence data are evaluated, including saturation densities, heat of vaporization, and vapor pressure. Both models perform well in describing the densities, but are no better than other molecular models in characterizing the vapor-liquid critical point, the heat of vaporization, and the vapor pressure. The QM/MM models are slightly better than others in describing the radial distribution functions, although it is clear that this QM polarization model can be further improved. The present study further demonstrates that a QM-based polarization model is a viable alternative to model polar fluids with strong intermolecular interactions. [DOI: 10.1063/1.1607919]

I. INTRODUCTION

The development of intermolecular potentials to mathematically model polar or associating molecules is of significant interest. One goal of the modeling effort is to predict thermodynamic properties at different state conditions based on the description of molecular interactions in statistical mechanical Monte Carlo (MC) and molecular dynamics (MD) simulations. The modeling approach is important for understanding the molecular origin of thermodynamic properties and has become a useful tool for predicting fluid behaviors at new conditions or at conditions that have no experimental information. The ability of a molecular model to capture properties ranging from the monomer level to the condensed bulk phase is essential to portray the fluid phase behavior accurately. At the bulk level a wide range of fluid properties are typically examined, e.g., vapor-liquid equilibrium (VLE) properties, radial distribution functions (RDF), volumetric properties, and heat effects.

Strong intermolecular bonding can arise in a molecular system when highly electronegative atoms are in the company of hydrogen atoms. Water, ammonia, and hydrogen fluoride (HF) are examples of molecules where such bonding occurs. Strong intermolecular interactions such as hydrogen bonding significantly influence the molecular structure, and thus small changes in the intermolecular bonding contributions to the energy can have a disproportionate effect on the bulk properties. Furthermore, electrostatic and hydrogen bonding interactions typically lead to significant many-body polarization effects that complicate the molecular modeling. The difficulty for a molecular model to capture properties beyond a narrow range of state conditions is closely related to the lack of a proper treatment of many-body polarization contributions. Although an increasing number of applications have utilized various polarizable models for condensed-phase systems of polar molecules,[1,2] the ability to capture the unique characteristics of polar species (such as water and hydrogen fluoride) through these treatments requires significant efforts.[3,4]

In comparison, quantum-mechanical (QM) models have not been widely used to represent molecular polarization in fluid simulations.[5,6] A complete description of fluid systems via full QM treatment remains practically impossible for such procedures as MC and MD simulations. The most routine implementation of a QM model is done through the Car–Parrinello approach[7] which hinges on the effectiveness[8] of the plane-wave density-functional theory (DFT) to model the molecular interactions. Another approach to apply QM-based models involves fitting of a parameterized potential surface to the results of two- and three-molecule QM calculations.[9] In a recent study we have examined the suitability of such models for describing the behavior of HF.[10] An alternative approach is the hybrid quantum-mechanical and molecular-mechanical (QM/MM) models[11,12] that combine advantages of both computational efficiency of classical

force fields and the accuracy of quantum-mechanical methods. As a result, the molecular-orbital derived polarization (MP) model was developed to describe molecular polarization for polar liquids,[5,6] making use of a novel implementation of the QM/MM scheme. As a test of principle, this approach has been applied to several molecular systems, including liquid water at temperatures of 25 and 100 °C. That study showed that the MP model can be parameterized to yield liquid properties, including density and heat of vaporization, in excellent agreement with experiments, and the performance of this electronic structure-determined polarization model is comparable to the best three-site empirical potentials. The model's unique characteristic is the ability to incorporate many-body effects through electronic structure methods. Much like the fluctuating charge model (FQ),[13] the wave function of individual molecules in the liquid and charge density depend upon the instantaneous state of the molecular system. However, the difference is that the charges are evaluated from molecular-orbital theory. As in the FQ model, the MP model represents molecular polarization by fluctuating charge densities (wave functions), in contrast to the traditional atomic point-dipole polarization model.[2,14]

Another important issue in modeling polar fluids is the treatment of intramolecular interactions. The experimental bond length of HF is certainly a function of the phase or state conditions. For example, solid-state calculations of DF estimate the bond length to be 0.95 Å at 85 K and 0.97 Å at 4.2 K.[15] Liquid phase calculations have produced estimates of 0.93 Å from pair correlation functions with corrections (for a monomer recoil in experiments) resulting in 0.95 Å.[16] Further, hexamer gas phase structures indicate the bond length of HF to be 0.973 Å.[17] Therefore a difficulty may arise for molecular simulation of HF when applying fixed bond lengths, or even variable bond lengths, at different state conditions. A monomer bond length must be chosen in simulation based on experimental properties, which in turn affects the magnitude of the permanent dipole moment. Two common choices for fixed bond length used in molecular simulation[2,18] of HF are 0.917 and 0.973 Å. Further, models have been developed to incorporate variable bond lengths to HF allowing for stretching through a Morse potential.[19]

We consider the ability of QM/MM potential model to describe the properties of vapor- and liquid-phase HF, applying the MP treatment and considering the effect of intramolecular bond length by examining two fixed HF bond length values: 0.973 and 0.917 Å. Theoretical background on this QM-based polarization model is presented in Sec. II, where the representation of the wave function for the electronic structure of the fluid is summarized and the MP Hamiltonian is formulated. Section III expands on the detailed simulation procedures and state conditions. Section IV presents results and insights from the study. Concluding remarks are made in Sec. V.

II. POTENTIAL MODEL

The implementation of a QM/MM model in molecular simulation of N species can be accomplished by making the assumption that the wave function of the fluid system, Φ, is represented by a Hartree product of the individual molecular wave functions of the solvent molecules Ψ_i,[5,6,12]

$$\Phi = \prod_{i=1}^{N} \Psi_i . \tag{1}$$

This leads to significant reduction in computational cost to a computationally manageable level by neglecting the exchange correlation interactions between different solvent molecules. However, the exchange correlation terms remain included in the representation of each solvent molecule, and the wave function for molecule i, Ψ_i, is represented by a Slater determinant of M doubly occupied orthonormal molecular orbitals ϕ_i:

$$\Psi_i = |\phi_1(1)\alpha(1)\phi_1(2)\beta(2)\cdots\phi_M(2M)\beta(2M)\rangle. \tag{2}$$

Here ϕ_i is a linear combination of N_b atomic basis functions χ_μ,

$$\phi_i = \sum_{\mu}^{N_b} c_{\mu i}\chi_\mu , \tag{3}$$

and is constrained by the orthonormality condition Λ_{ij}:

$$\Lambda_{ij} = \sum_{\mu}^{N_b} c_{\mu i}c_{\mu j} - \delta_{ij} = 0. \tag{4}$$

The molecular-orbital coefficients $c_{\mu i}$ are evaluated through a typical Hartree–Fock iterative procedure using a combined QM/MM effective Hamiltonian (see below).[5,6,12]

A further reduction in computational cost is achieved by making use of the ideas of combined QM/MM methods. Specifically, in determining the individual molecular wave function, we treat the surrounding solvent molecules by a set of classical point charges derived from their corresponding wave functions, which, in turn, are influenced and polarized by the interactions with other molecules. Thus an iterative, self-consistent procedure is carried out to achieve an overall system convergence. Once Φ is established, the definition of the energy terms of the system can be conveniently formulated.

To begin the energy formulation, we define the Hamiltonian of the fluid system as follows:

$$\hat{H} = \sum_{i=1}^{N} \hat{H}_i^{\circ} + \tfrac{1}{2}\sum_{i=1}^{N}\sum_{j\neq i}^{N} \hat{H}_{ij} , \tag{5}$$

where $\hat{H}_i^{\circ}$ is the Hamiltonian for an isolated molecule i, and $\hat{H}_{ij}$ represents Coulombic interactions between molecules i and j. By making the assumption that there is no electron transfer between different molecules, the Coulombic interaction Hamiltonian, $\hat{H}_{ij}$ can be reduced to a form that is computationally convenient for molecular simulations,

$$\hat{H}_{ij}(\Psi_j) = -\sum_{a=1}^{2M} V_a(\Psi_j) + \sum_{\alpha=1}^{A} Z_\alpha(i)V_\alpha(\Psi_j), \tag{6}$$

where A is the total number of atoms in a solvent molecule, $Z_\alpha(i)$ is the nuclear charge of atom α, and $V_x(\Psi_j)$ is the electrostatic potential of monomer j at either the electronic or nuclear positions of molecule i. Explicitly, the first term is the interaction of molecule j's electrons and nuclei with mol-

TABLE I. Parameters used at two different FH bond lengths r_{FH}. Parameters σ_{ij} and ε_{ij} are selected to equal those for two prominent potential models for HF, JVP (Ref. 2), and CJ84 (Ref. 20), having corresponding H–F bond lengths. K represents a Mulliken population scaling factor of charges, which is fit to experimental densities at 300 K and 2 bars.

	JVP	MP(AM1)	CJ84	MP(AM1)
r_{FH}, Å	0.973	0.973	0.917	0.917
σ_{FF}, Å	3.05	3.05	2.984	2.98
σ_{HH}, Å		0.800		0.800
ε_{FF}, kcal/mol	0.21857	0.21857	0.151	0.150
ε_{HH}, kcal/mol		0.05		0.05
K		1.475		1.475

ecule i's *electrons* and the second term represents the interactions of molecule j's electrons and nuclei with molecule i's *nuclei*.

If the electrostatic potential $V_x(\Psi_j)$ is determined approximately by a set of point charges $q_\beta(\Psi_j)$ derived from the wave function Ψ_j, Eq. (6) reduces to

$$\hat{H}_{ij}(\Psi_j) = -\sum_{a=1}^{2M}\sum_{\beta=1}^{A}\frac{q_\beta(\Psi_j)}{r_{\alpha\beta}} + \sum_{\alpha=1}^{A}\sum_{\beta=1}^{A}\frac{Z_\alpha(i)q_\beta(\Psi_j)}{R_{\alpha\beta}} + E_{ij}^{\mathrm{vdW}}, \tag{7}$$

where $r_{\alpha\beta}$ is the distance between an electron of molecule i and molecule j, and $R_{\alpha\beta}$ is the distance between nuclear centers of atoms of molecule i and molecule j. In Eq. (7), a van der Waals (vdW) term E_{ij}^{vdW} is added, expressed here in terms of the Lennard-Jones (LJ) potential to represent short-range exchange repulsion interactions that have been neglected in the definition of the wave function of the system by Eq. (1) and long-range dispersion interactions not included in the Hartree–Fock approximation:

$$E_{ij}^{\mathrm{vdW}} = \sum_{\alpha=1}^{A}\sum_{\beta=1}^{A} 4\varepsilon_{\alpha\beta}\left[\left(\frac{\sigma_{\alpha\beta}}{R_{\alpha\beta}}\right)^{12} - \left(\frac{\sigma_{\alpha\beta}}{R_{\alpha\beta}}\right)^{6}\right]. \tag{8}$$

The parameters $\sigma_{\alpha\beta}$ and $\varepsilon_{\alpha\beta}$ in Eq. (8) will be determined by a fitting procedure with primary interest in experimental bulk phase properties (Table I).

The total potential energy of the system is given as the expectation value. For convenience, we define the zero of the energy by a system of infinitely separated solvent molecules. Consequently, the total interaction energy of the fluid system is given by

$$E_{\mathrm{tot}} = \langle\Phi|\hat{H}|\Phi\rangle - N\langle\Psi^\circ|\hat{H}_i^\circ|\Psi^\circ\rangle. \tag{9}$$

The second term of the energy is the reference energy of N isolated molecules with Ψ° representing the wave function of a molecule in the gas phase.

Because of the partition of the system in combined QM/MM treatment in which one molecule is treated explicitly by quantum mechanics and the rest is approximated by a set of partial charges, the interaction Hamiltonian $\hat{H}_{ij}$ is not identical to $\hat{H}_{ji}$, yet, they represent the same interactions between molecules i and j.[5,6,12] This inherent imbalance in combined QM/MM calculations is not a problem in calculating the total interaction energy using Eq. (9), but it is convenient to define explicitly the pair interaction energy as the average of the two interaction Hamiltonians,[5,6,12]

$$E_{ij} = \tfrac{1}{2}[\langle\Psi_i|\hat{H}_{ij}|\Psi_j\rangle + \langle\Psi_j|\hat{H}_{ji}|\Psi_i\rangle]. \tag{10}$$

The use of atomic partial charges to represent the electrostatic potential in Eq. (7) is a rather crude approximation, although it can be exactly described if a full multipole expansion approach is used. For computational convenience, we found that the truncation at the monopole term is reasonable in the study of liquid water, provided that the partial charges $q_\beta(\Psi_j)$ derived from Mulliken population analysis are scaled. It turns out that a single scaling parameter is sufficient to yield reasonable results for simple liquids,

$$q_\beta(\Psi_j) = KQ_\beta^M, \tag{11}$$

where K is optimized to fit fluid properties. The atomic charges are determined specifically from applying the neglect of diatomic differential overlap (NDDO) approximation to give

$$Q_\beta^M = Z_\beta(j) - 2\sum_{a=1}^{M}\sum_{\mu\in\alpha} c_{\mu a}(j)^2, \tag{12}$$

where $c_{\mu i}$ are determined through the solution of the Hartree–Fock equation. In this way, $q_\beta(\Psi_j)$ is self-consistent and is comprehensively defined by Ψ_j.

Given an initial molecular configuration and $c_{\mu i}$, the above equations are converged to an energy for the N-molecule fluid system. Typically $c_{\mu i}$ is taken from a previous step during the MC or MD simulation. The initial guess for the orbital coefficients can be taken from the gas phase wave function. Next, atomic partial charges $q_\beta(\Psi_j)$ are calculated from Ψ_j and incorporated in the formation of the Fock matrix through the Hamiltonian in Eq. (5). The Hartree–Fock equations are solved to produce a new set of $c_{\mu i}$ which are in turn used to calculate and test the convergence of the energy. The procedure is repeated until the total energy of the system converges.

III. SIMULATION DETAILS

Two parameter sets, σ_{ij}, ε_{ij} and K, were developed for the MP model for hydrogen fluoride, corresponding to two r_{FH} values, 0.917 and 0.973 Å. In Table I, the LJ parameters are presented with those of the models of Jedlovzsky and Vallauri (JVP),[2] and Cournoyer and Jorgensen (CJ84).[20] The LJ fluorine parameters, σ_{ij}, ε_{ij}, were fixed to be the values described in corresponding JVP/CJ84 models, while the hydrogen parameters are those given in the QM/MM model of water.[5] The semiempirical Austin model 1 (AM1) method is used to describe the molecular wave function for hydrogen fluoride.[21] The charge-scaling parameter K was adjusted until the Monte Carlo simulations yield results in good agreement with experiments on liquid density and energy at 300 K and 2 bars. In regard to the present development it is helpful to understand where the polarization effects appear in the JVP and CJ84 models: JVP includes explicit polarization energies

(through induced dipole effects), while CJ84 applies polarization in a pairwise-effective way (through an exaggerated permanent dipole moment).

We assess the MP model in conjunction with the effects of different HF monomer bond lengths, r_{FH}, through comparison with experimental fluid phase properties. Recently, Pfleiderer *et al.*[22] determined experimentally the structure of HF at six state points, including two liquid states and four supercritical states. In addition, the experimental densities[23] at the same states allow for a general analysis of the accuracy of the MP model. Molecular simulation calculations of density values and RDFs at two of the Pfleiderer *et al.* state conditions (liquid at 300 K and 2 bars, and supercritical fluid at 473 K and 78 bars) give a good picture of the strengths and deficiencies of a molecular interaction model. Density calculations of the model were accomplished through a simulation in the NPT ensemble while the RDFs were measured in the canonical (NVT) ensemble. Additionally, dipole moments were averaged throughout both NPT and NVT simulations and compared to each other. For each condition, 216 HF molecules were simulated through 5×10^6 configurations. The NVT simulations consisted of only displacement/rotation moves. The NPT simulations additionally consisted of one volume move per 216 displacement/rotation moves.

Another assessment of the MP model and the r_{FH} parameter is accomplished through comparison with VLE experimental properties. Saturated densities, saturated vapor pressures and heat of vaporizations were calculated through Gibbs ensemble (GE) molecular simulations. The saturated vapor pressures were evaluated through the methodology of Harismiadis *et al.*[24] The calculated saturated densities and saturated vapor pressures yielded heats of vaporization through direct calculation,

$$\Delta H^{\mathrm{vap}}=\langle U^{\mathrm{vap}}\rangle-\langle U^{\mathrm{liq}}\rangle+\langle P^{\mathrm{sat}}\rangle\left(\frac{1}{\langle\rho_{\mathrm{vap}}\rangle}-\frac{1}{\langle\rho_{\mathrm{liq}}\rangle}\right). \qquad (13)$$

Specifics of the GE simulations include a simulation length of 5×10^4 cycles, each of which consists of 216 MC moves, at each state point, system size of 216 molecules, and averaging block size of 1000 cycles for error analysis.

All interactions were truncated at an F–F separation of 9 Å and the only treatment for truncation applied was the standard Lennard-Jones long-range correction. In particular no long-range correction to the electrostatic interactions (e.g., Ewald sum) was applied. This choice results in considerable savings in computation. Previous studies by us and others[10,25] have found that neglect of long-range electrostatics does not greatly affect the phase coexistence and structural properties for highly orientationally specific hydrogen bonding systems such as HF and water.

IV. RESULTS AND DISCUSSION

Densities and molecular dipole moments measured by the simulation are listed in Table II, and RDFs are presented in Figs. 1 and 2, as calculated for a liquid at 300 K and 2 bars, and a supercritical fluid at 473 K and 78 bars. Computational results can be directly compared with experimental data for these two state points. Since the liquid at 300 K and 2 bars was chosen as the calibration point of the MP model, the calculated simulation densities in Table II reveals the success of the fit (to experiment).

TABLE II. Calculated densities at chosen state conditions via MC NPT simulations. Calculated dipole moments $\langle\mu_{HF}\rangle^{NPT}$ and $\langle\mu_{HF}\rangle^{NVT}$, at chosen conditions via MC NVT and NPT simulations. The $\langle\mu_{HF}\rangle^{NPT}$ and $\langle\mu_{HF}\rangle^{NVT}$ values are compared with an experimental gas phase dipole moment (Ref. 26), μ°_{HF}, of 1.82 D.

	Density NPT (g/cm^3)	
r_{FH}, Å	300 K, 2 bars	473 K, 78 bars
0.917	0.9529±0.0006	0.0507±0.0007
0.973	0.9554±0.0044	0.0477±0.0005
Expt.	0.962	0.236
r_{FH}, Å	$\langle\mu_{HF}\rangle^{NPT}$ (D)	
	300 K, 2 bars	473 K, 78 bars
0.917	1.9863±0.0006	1.7890±0.0003
0.973	2.0320±0.0006	1.7890±0.0003
r_{FH}, Å	$\langle\mu_{HF}\rangle^{NVT}$ (D)	
	300 K, 0.962 g/cc	473 K, 0.236 g/cc
0.917	1.9853±0.0006	1.8479±0.0007
0.973	2.0316±0.0006	1.8804±0.0004

Inspection of Table I shows an increase in the average dipole moments $\langle\mu_{HF}\rangle$ at the liquid phase when compared to the gas phase dipole moment μ°_{HF}. In the condensed phase, the magnitude of $\langle\mu_{HF}\rangle$ exemplifies the degree of polarization. The optimized bond length for HF using AM1 is 0.826 Å, which is too short compared with experiments. Using either a r_{FH} value of 0.917 or 0.973 Å, which have been used in other empirical models for hydrogen fluoride, the computed dipole moment in the gas phase is 0.69 and 0.70 D, respectively. This is significantly smaller than the experimen-

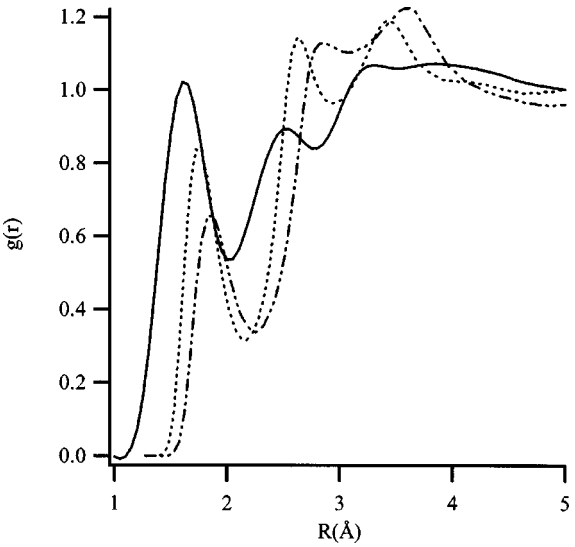

FIG. 1. Combined radial distribution function (RDF) calculated from NVT simulations, 300 K and 2 bars, and compared to experimental data of Pfleiderer *et al.* (Ref. 22). The combination of atomic RDFs calculated from simulation yields the total RDF, $g(r)$, through $0.4966g_{FH}+0.2104g_{FF}+0.2930g_{HH}$ (Ref. 22). Double broken lines correspond to r_{FH} equal to 0.973 Å and single broken lines correspond to r_{FH} equal to 0.917.

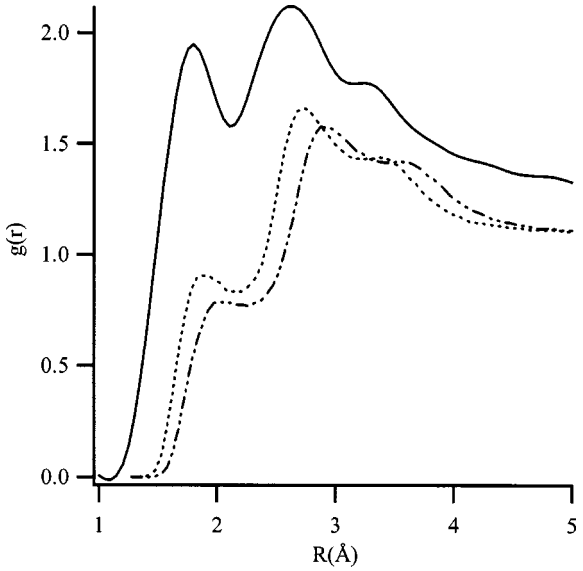

FIG. 2. Same as Fig. 1 but at 473 K and 78 bars (supercritical).

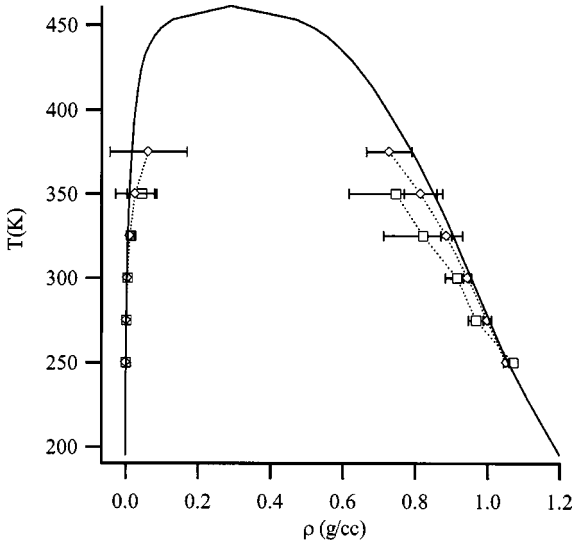

FIG. 3. Vapor–liquid coexistence densities, ρ^{vap} and ρ^{liq}, as calculated from Gibbs ensemble (GE) simulations (open markers) and compared to experiment (solid line) (Ref. 28). Squares show calculation for r_{FH} equal to 0.917 Å and diamonds show calculations for r_{FH} equal to 0.973 Å.

tal value[26] of 1.82 D, suggesting that the AM1 model has a very strong covalent character in the molecule HF, which is also reflected by the need to use a *K* value of 1.475 to enhance the computed charge separation. The liquid HF at 300 K, the computed average dipole moment is 1.99 ± 0.01 D and 2.03 ± 0.01 D for the two HF geometries. This represents a significant increase in molecular polarization, with a net induced dipole moment of about 1.3 D. At supercritical conditions, the dipole moment and polarization is somewhat reduced to a value of about 1.79 D, still a major enhancement over the gas phase value (1.1 D). This suggests that HF is strongly hydrogen bonded in the supercritical states.

It is interesting to compare the computed densities in the liquid state at 300 K and at the supercritical point, 473 K. The densities of both r_{FH} geometries in Table II show less satisfactory agreement to experimental results for the supercritical state. Disagreement in density values of many HF potential models (with experiment) at this supercritical condition is not uncommon.[4] Furthermore, similar statements about the change in the simulation dipole moment can be made in regard to the deviation of the supercritical RDF from experiment when Fig. 2 is examined (these were calculated at the experimental density, so their poor comparison is not a consequence of the density behavior).

The computed radial distribution functions (RDFs) in Fig. 1 show better structural properties for the model of $r_{FH} = 0.917$ Å in comparison to the model with $r_{FH} = 0.973$ Å. The first peak is more prominent in for the 0.917 model. In both cases, however, the RDFs indicate repulsion that is a bit too strong in comparison to experimental behavior.

VLE results are now compared for the two proposed parameter sets; data are presented in Figs. 3–6. The coexistence densities for $r_{FH} = 0.973$ Å parameter set shows improvement relative to the shorter r_{FH} in comparison to experiment. Calculated vapor pressures also show the same improvements when the two parameter sets are compared, although both consistently exceed the experimental values. As with almost every interaction model we have studied, the heat of vaporization of both parameter sets shows very poor agreement with experiment. Likewise the critical point is in both cases is much smaller than that determined experimentally.

All comparisons between simulation and experiment are consistent with a vapor phase model that underestimates molecular association and clustering. This is apparently an intrinsic problem of the semiempirical AM1 model, which is too strong in covalent character as indicated by the computed dipole moment in the gas phase. Stronger vapor phase clustering would lower the vapor pressure and heat of vaporization, which would, in turn, increase the vapor density and enhance the structural features. The behavior of the two

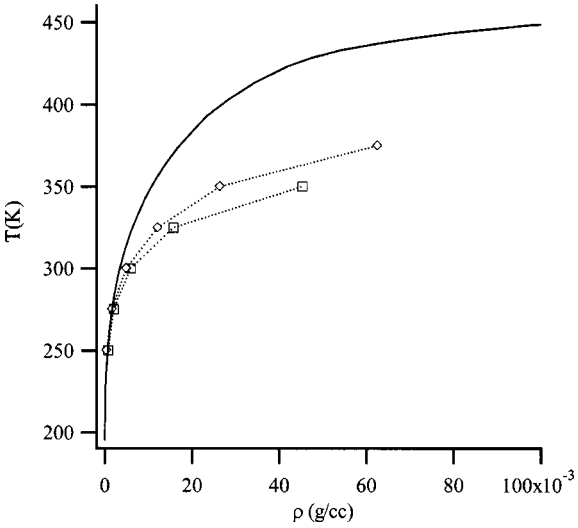

FIG. 4. VLE vapor coexistence densities ρ^{vap} from GE simulations (open markers) and compared to experiment (solid line) (Ref. 28). Squares show calculation for r_{FH} equal to 0.917 Å and diamonds show calculations for r_{FH} equal to 0.973 Å.

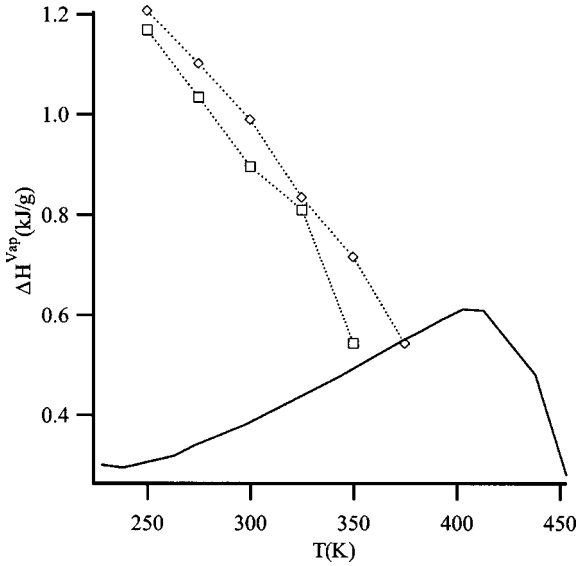

FIG. 5. Heats of vaporization ΔH^{vap} as calculated from GE simulations (open markers) and compared to experiment (solid line) (Ref. 28). Squares show calculation for r_{FH} equal to 0.917 Å and diamonds show calculations for r_{FH} equal to 0.973 Å.

models differs, but not by a magnitude needed to bring the properties in line with experiment. Better cohesion is required, perhaps by reducing the van der Waals radius that was developed for the CJ84 empirical model and softening repulsive interactions. Features are needed to enable the model to adapt properly to changes in density—and polarization is not the only consideration in this direction. The performance of the present model may be improved by reparameterizing the semiempirical model for the fluorine atom. The only evidence of an experimental r_{FH} equal to 0.973 Å is given through neutron-scattering experiments focusing particularly on the gas phase hexamer ring structure,[17] while other experiments[16,22,27] indicate shorter bond lengths are appropriate. So, it seems that the best modeling approach may require a variable r_{FH} molecular model to describe the HF molecule.

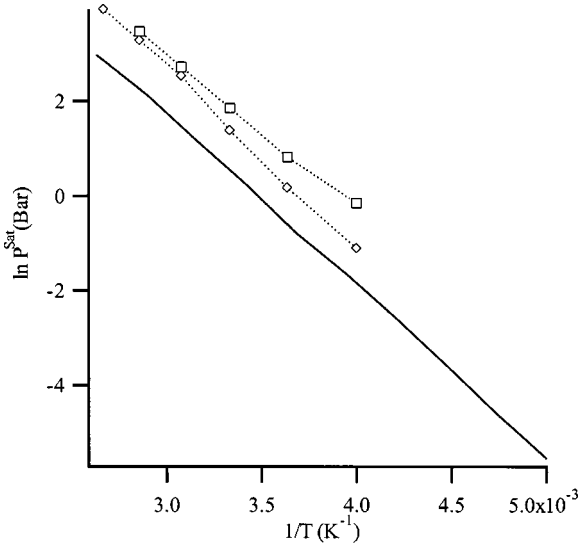

FIG. 6. Vapor pressures P^{sat} as calculated from GE simulations (open markers) through Harismiadis *et al.* methodology (Ref. 24) and compared to experiment (solid line) (Ref. 28). Squares show calculation for r_{FH} equal to 0.917 Å and diamonds show calculations for r_{FH} equal to 0.973 Å.

V. CONCLUSION

An analysis of the MP formulation in conjunction with two different intramolecular bondlength values for HF was conducted through the parameterization to a liquid phase density at 300 K and 2 bars. The description of structural and fluid phase properties by the model have been considered in comparison to experiment. The densities, RDFs, and dipole moments were measured by simulation over two chosen state conditions, one a liquid state and the other a supercritical state. Also, the coexistence densities, vapor pressures, and heat of vaporization were evaluated through Gibbs ensemble simulations. The scope of the work allows for detailing the impact of a variation in bond lengths on fluid phase properties. The simulations for r_{FH} equal to 0.973 Å shows slight improvements in the VLE, relative to the behavior of the shorter-bond model, but is poorer in its structural properties. Analysis of the average dipole moment shows the importance of correctly describing the change of polarization effects with fluid conditions. The present study demonstrates that there is significant fluid phase polarization effect in both liquid and supercritical fluid HF and that this effect can be modeled by a potential function based on electronic structure theory. Although the computed thermodynamic and structural results are reasonable for the ambient conditions, significant deviation from experimental data at the supercritical state still exists. This is attributed to the intrinsic weak polar character of the AM1 model for HF. The present model may be further improved by readjusting the semiempirical parameters for the fluorine atom, and by consistent optimizations of both the Lennard-Jones parameters and the charge scaling constant.

ACKNOWLEDGMENTS

This work was supported in part by the National Science Foundation, Grant No. CTS-0076515 (D.A.K.), and the National Institutes of Health (J.G.). Computing facilities were provided by the University at Buffalo Center for Computational Research.

[1] M. W. Mahoney and W. L. Jorgensen, J. Chem. Phys. **112**, 8910 (2000); J. L. Rivera, M. Predota, A. A. Chialvo, and P. T. Cummings, Chem. Phys. Lett. **357**, 189 (2002); H. A. Stern, F. Rittner, B. J. Berne, and R. A. Friesner, J. Chem. Phys. **115**, 2237 (2001); J. Gao, D. Habibollazadeh, and L. Shao, J. Phys. Chem. **99**, 16460 (1995); J. Gao, J. J. Pavelites, and D. Habibollazadeh, *ibid.* **100**, 2689 (1996).
[2] P. Jedlovszky and R. Vallauri, J. Chem. Phys. **107**, 10166 (1997).
[3] M. Lisal, J. Kolafa, and I. Nezbeda, J. Chem. Phys. **117**, 8892 (2002); P. Jedlovszky and R. Vallauri, Mol. Phys. **92**, 331 (1997).
[4] P. Jedlovszky, M. Mezei, and R. Vallauri, J. Chem. Phys. **115**, 9883 (2001).
[5] J. Gao, J. Chem. Phys. **109**, 2346 (1998).
[6] J. Gao, J. Phys. Chem. B **101**, 657 (1997).
[7] A. J. Sillanpaa, C. Simon, M. L. Klein, and K. Laasonen, J. Phys. Chem. B **106**, 11315 (2002); S. Izvekov and G. A. Voth, J. Chem. Phys. **116**, 10372 (2002); R. Car and M. Parrinello, Phys. Rev. Lett. **55**, 2471 (1985).
[8] S. Tsuzuki and H. P. Luthi, J. Chem. Phys. **114**, 3949 (2001).
[9] W. Klopper, M. Quack, and M. A. Suhm, J. Chem. Phys. **108**, 10096

(1998); M. Quack, J. Stohner, and M. A. Suhm, J. Mol. Struct. **599**, 381 (2001).
[10] S. Wierzchowski and D. A. Kofke, J. Chem. Phys. (to be published).
[11] G. A. Kaminski and W. L. Jorgensen, J. Phys. Chem. B **102**, 1787 (1998); N. Reuter, A. Dejaegere, B. Maigret, and M. Karplus, J. Phys. Chem. A **104**, 1720 (2000); A. Warshel and M. Levitt, J. Mol. Biol. **103**, 227 (1976); M. J. Field, P. A. Bash, and M. Karplus, J. Comput. Chem. **11**, 700 (1990).
[12] J. Gao, Rev. Comput. Chem. **7**, 119 (1996).
[13] J. L. Banks, G. A. Kaminski, R. H. Zhou, D. T. Mainz, B. J. Berne, and R. A. Friesner, J. Chem. Phys. **110**, 741 (1999); H. A. Stern, G. A. Kaminski, J. L. Banks, R. H. Zhou, B. J. Berne, and R. A. Friesner, J. Phys. Chem. B **103**, 4730 (1999).
[14] I. M. Svischchev, P. G. Kusalik, J. Wang, and R. J. Boyd, J. Chem. Phys. **105**, 4742 (1996).
[15] M. W. Johnson, E. Sandor, and E. Arzi, Acta Crystallogr., Sect. B: Struct. Crystallogr. Cryst. Chem. **B31**, 1998 (1975).
[16] M. Deraman, J. C. Dore, J. G. Powles, J. H. Holloway, and P. Chieux, Mol. Phys. **55**, 1351 (1985).
[17] J. Janzen and L. S. Bartell, J. Chem. Phys. **50**, 3611 (1969).
[18] M. E. Cournoyer and W. L. Jorgensen, Mol. Phys. **51**, 119 (1984); P. Jedlovszky and R. Vallauri, *ibid.* **93**, 15 (1998); M. L. Klein, I. R. McDonald, and S. F. O'Shea, J. Chem. Phys. **69**, 63 (1978).
[19] R. G. Della Valle and D. Gazzillo, Phys. Rev. B **59**, 13699 (1999).
[20] M. E. Cournoyer and W. L. Jorgensen, Mol. Phys. **51**, 119 (1984).
[21] M. J. S. Dewar, E. G. Zoebisch, E. F. Healy, and J. J. P. Stewart, J. Am. Chem. Soc. **107**, 3902 (1985).
[22] T. Pfleiderer, I. Waldner, H. Bertagnolli, K. Todheide, and H. E. Fischer, J. Chem. Phys. **113**, 3690 (2000).
[23] E. U. Franck and W. Spalthoff, Z. Elektrochem. **61**, 348 (1957); E. U. Franck, G. Wiegand, and R. Gerhardt, J. Supercrit. Fluids **15**, 127 (1999).
[24] V. I. Harismiadis, J. Vorholz, and A. Z. Panagiotopoulos, J. Chem. Phys. **105**, 8469 (1996).
[25] I. Nezbeda and J. Kolafa, Mol. Phys. **97**, 1105 (1999).
[26] D. R. Lide, *CRC Handbook of Chemistry and Physics: A Ready-Reference Book of Chemical and Phyical Data*, 71st ed. (CRC, Boca Raton, FL, 1990).
[27] G. Herzberg, *Molecular Spectra and Molecular Structure. I. Diatomic Molecules*, 2nd ed. (Van Nostrand, New York, 1955).
[28] C. P. C. Kao, M. E. Paulaitis, G. A. Sweany, and M. Yokozeki, Fluid Phase Equilib. **108**, 27 (1995).